PHOTOMETRIC SYSTEM DESIGN AND PERFORMANCES

C. Jordi[1,2]**, E. Høg**[3]

[1]Dept. Astronomia i Meteorologia, Universitat de Barcelona, Avda. Diagonal 647, E-08028 Barcelona, Spain
[2]IEEC, Gran Capità, 2-4, E-08034 Barcelona, Spain
[3]Copenhagen University Observatory, Juliane Maries Vej 30, DK-2100 Copenhagen Ø, Denmark

ABSTRACT

If unsupported by appropriate diagnostic data, Gaia would yield immense numbers of positions and velocities of objects whose astrophysical nature would be unknown. The core science case requires measurement of luminosity, effective temperature, mass, age and chemical composition for the stellar populations in the Galaxy and its nearest neighbours. These quantities can be derived from the spectral energy distribution of the stars, i.e. through high-quality multi-band photometry. The current proposals for broad and medium band photometric systems, their capabilities for the astrophysical parametrization of the stars and hence the expected precision of the stellar populations characterization are reviewed.

Key words: Gaia; Photometry; Galactic astronomy; Stellar classification.

1. INTRODUCTION

After five years of scanning the entire sky, Gaia will have observed about one billion objects down to $V_{\rm lim} \sim 20 - 26$. The photometric measurements are indispensable in providing the basic tools for classifying those objects as stellar or non-stellar and for parametrizing them according to their nature. Classification and parametrization across the entire Hertzsprung-Russell diagram has to be feasible as well as the identification of peculiar objects. To achieve this it is necessary to observe a large spectral domain, extending from the ultraviolet to the infrared. The photometric measurements must be able to determine (i) effective temperatures and reddening at least for OBA stars (needed both as tracers of Galactic spiral arms and as reddening probes), (ii) at least effective temperatures and abundances for late-type giants and dwarfs, and (iii) luminosities for stars having large relative parallax error, and all of this with an accuracy sufficient for the quantitative description of the chemical and dynamical evolution of the Galaxy over all galactocentric distances.

To be able to reconstruct Galactic formation history the distribution function of stellar abundances must be determined to ~ 0.2 dex, while effective temperatures must be obtained to ~ 2 per cent. These yield an uncertainty of ~ 2 Gyr in the age determination. The same precisions allow separation of stars belonging to different populations (i.e., disc and halo stars, and also thin and thick disc populations). Separate determination of abundance of Fe and α-elements will be essential for mapping Galactic chemical evolution.

Photometry is also necessary to account for the chromatic aberrations in the astrometric focal plane to achieve the microarcsec accuracy level.

This paper reviews the capabilities of the current Gaia photometric systems and the estimated accuracies of the derived stellar parameters. The paper is the result of the contributions by many members of the Photometry Working Group.

2. INSTRUMENT DESCRIPTION

Briefly, the Gaia satellite will perform photometric measurements by means of two physically separated telescopes: the Astro instrument, which is primarily designed for astrometric observations, and the Spectro instrument, primarily used for photometry and radial-velocity measurements. The two instruments differ widely in spatial resolution, available integration time, and the number and type of filter bands that can be used.

The astrometric focal plane is basically divided into two fields. One for the detection, confirmation and astrometric measurements themselves and a second one devoted to broad-band photometric measurements.

The accuracy of the astrometry is higher as the signal increases and therefore the astrometric field is not equipped with any filter, i.e., it measures white light. The associated very broad-band magnitude, G, defined by the wavelength coverage of the CCDs ($\sim$ 400 – 1000 nm), is described in Section 3.

In order to attain the nominal astrometric accuracy desired for Gaia, measurements must be compensated for

the residual chromaticity. This is only possible with the knowledge of the spectral energy distribution of each observed target in the wavelength range covered by the CCDs. This is the main purpose of the broad-band photometry (BBP), described in Section 4.1.

The Spectro focal plane is entirely devoted to the medium-band photometry (MBP) and its goal is to determine stellar astrophysical parameters to enough accuracy for the understanding of the composition, formation and evolution of the Milky Way. As stated above, this is done through accurate determinations of abundances and ages. The MBP is described in Section 4.2.

All observations are made with CCDs operating in TDI (drift-scanning) mode, i.e., with the charge image transported in synchrony with the optical image moving across the field due to the rotation of the satellite. The rotation speed is fixed giving a fixed integration time per CCD crossing, depending on the angular size of the CCD on the sky. Each CCD may be equipped with an interference filter defining (together with the mirrors and the CCD) a certain photometric band. Half of the CCDs in the Spectro focal plane are blue sensitive and half of them are red sensitive, in order to yield the maximum signal-to-noise ratio in all the wavelength coverage.

Data from the CCDs are only sampled in certain 'windows', i.e., areas centred on each detected star. In this way the read-out noise and the amount of data to be transmitted to ground are reduced. The current schemes of sampling are described in Høg (2004a) and Høg (2004b).

3. THE G MAGNITUDE

Astrometric observations will be performed in white light (corresponding to a very broad band $\sim$ 400 – 1000 nm). The associated G magnitude relates with Johnson V magnitude as shown in Figure 1. In the case of very red objects, they are about 6 magnitudes brighter in G than in V, and therefore, the Gaia limiting magnitude of $G_{\rm lim} \sim 20$ translates into $V_{\rm lim} \sim 20 - 26$, depending on the colour of the observed object. This very broad-band magnitude, and its time dependence, can be obtained from the analysis and rigorous calibration of the primary mission data (i.e., by determination of the amplitudes as well as the phase of the astrometric focal plane image). The G magnitude yields the best S/N for variability detection among all instruments on board Gaia. The estimated precisions are given in Figure 2 for each transit and at the end of the mission.

When combined with the parallax (and an estimate for the interstellar absorption), G gives a measure of the absolute magnitude. Gaia will ultimately provide absolute magnitudes for 180 million stars. And, as Hipparcos did, Gaia will discover eclipsing binaries, Cepheids, RR Lyrae, etc. The precision of the light curves at the end of the mission (with an average of 82 observations) for variable stars with $V \sim 20$ is similar to those of Hipparcos at $V \sim 9$. The Cepheids in the LMC ($V \sim 13.5{-}16.5$) will be measured with single transit precision at the level of

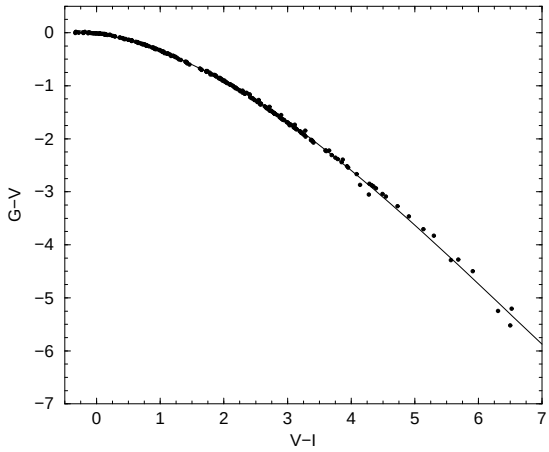

Figure 1. Colour-colour relation providing the G magnitude associated to the white light in the astrometric focal plane.

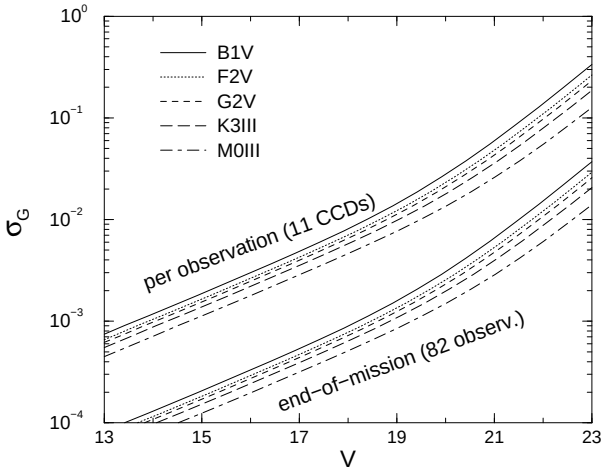

Figure 2. Estimated precision of the G magnitude per passage and at the end of the mission without considering a minimum threshold error coming from the calibration of the mission. This minimum error is assumed to be about 3 mmag.

the calibration errors and those in M31 ($V \sim 19.5{-}22.5$) with precision from 0.015 to 0.15 mag.

4. BROAD AND MEDIUM BAND PHOTOMETRIES

Many ground-based photometric systems exist but none satisfy all the requirements of a space-based mission such as Gaia: portions of the spectrum limited on-ground by terrestrial atmospheric O_3 and H_2O bands are opened up to Gaia; classical photometric systems are designed for specific spectral type intervals or specific objects, while Gaia must cover the entire Hertzsprung-Russell diagram, quasar and galaxy photometry, Solar System objects classification, and many more diverse objects. In addition,

Gaia allows the extension of stellar photometry to galactic areas where the classical classification schemes are no longer fully valid because of systematic variations in element abundances in stellar atmospheres and in interstellar matter.

Considerable effort is being devoted to the design of optimum broad-band (BBP) and medium-band (MBP) filter systems, taking into account the spectral energy distribution of the primary targets of Gaia, i.e., those types of stars crucial for achieving the core science case. Different approaches are being used. Munari (1999), Grenon et al. (1999), Vansevicius & Bridzius (2003), Lindegren (2003a), Straižys et al. (2004), Knude & Høg (2004) and Jordi et al. (2004b) base their proposals on their current expertise and performances of known photometric systems, while Bailer-Jones (2004) and Heiter et al. (2004) derive the optimal location and width of the bands by using the Heuristic Filter Design code and Principal Component Analysis, respectively.

4.1. BBP

The basic transmittance curve of the interference filters versus wavelength is a symmetric quasi-trapezoidal shape. Lindegren (2003c) showed that for chromaticity, near rectangular filters are acceptable and that the choice of the separation wavelengths is more important than the edge widths. The author concludes that four broad bands are enough to match the chromaticity constraints (r.m.s. residuals < 5 μas).

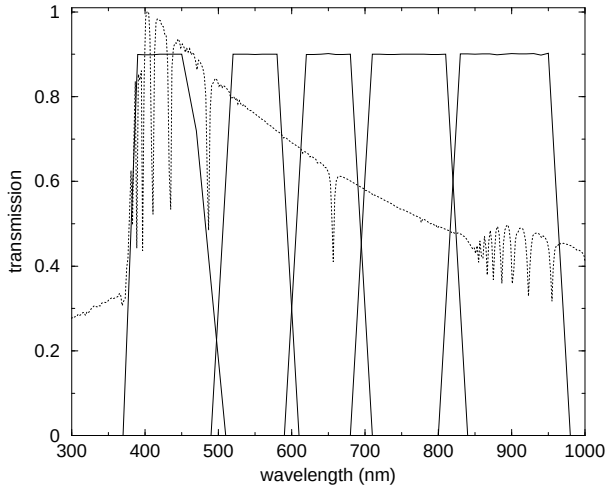

Figure 3. The V1B BBP system is overplotted on the spectral energy distribution of an A0 V star (dotted line)

With an angular resolution better than that of the MBP, the BBP will be crucial for astrophysics in the cases of close pairs and crowded fields. This is important for areas of the sky with a stellar density larger than 50 000 – 100 000 stars per deg^2. These regions cannot be observed satisfactorily with the medium-band photometry system due to the angular resolution of the Spectro telescope. To obtain the maximum astrophysical return, five bands are preferred to four, and most of the current proposals are considering five filters like the ones by Lindegren (2003a), Straižys (2004) and Jordi & Carrasco (2004a). Figure 3 shows the best performing system at present. The system behaves similarly to the $BVRI$ Johnson system in terms of derivation of astrophysical quantities. Other systems under evaluation intend to improve the luminosity determination of early-type stars.

As an example of the attainable precisions, Figure 4 shows the estimated error of magnitudes as a function of V apparent magnitude and spectral type for the V1B proposal.

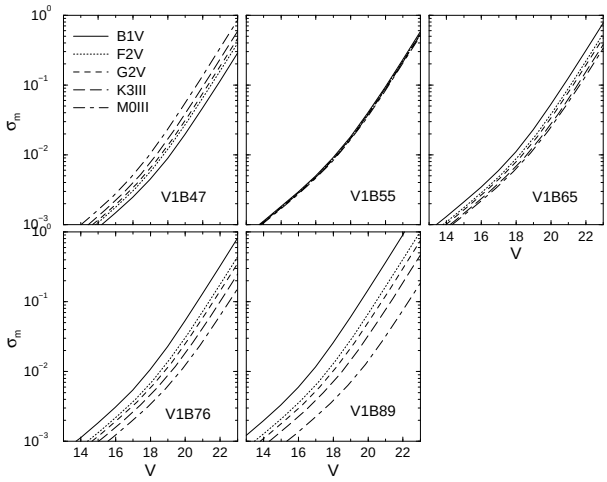

Figure 4. Estimation of the end-of-mission precisions for the five bands in the V1B proposal by Straižys (2004) as a function of V apparent magnitude and spectral type without considering a minimum threshold error coming from the calibration of the mission. This minimum error is assumed to be about 3 mmag. The central wavelength of the filter is indicated by the last digits in the name.

4.2. MBP

As stated above, the MBP aims to classify the observed objects (star, solar system body, QSO, ...) and to characterize them in terms of astrophysical parameters (i.e., $T_{\rm eff}$, luminosity or $\log g$, [M/H], anomalies, emission, ...).

To ensure this, several bands are devoted to measuring the continuum, indicative of the effective temperature and interstellar absorption, and others to measuring the spectral features sensitive to luminosity and/or abundances. The ultraviolet domain contains the most useful information on gravity and interstellar reddening for OBA-type stars, and on metallicity for FGK-type stars. In the interval 375 – 445 nm, most lines belong to iron peak elements but there are also CN bands, strong CaII lines, the Q and R branches of CH radical and the P branch, although this is less intense. This range is especially important for metallicity determination for FGK stars. The Mg/MgH feature at 510 nm is sensitive to gravity for late type stars and to Mg abundances. The red part of the available spectral range is dominated by the TiO bands

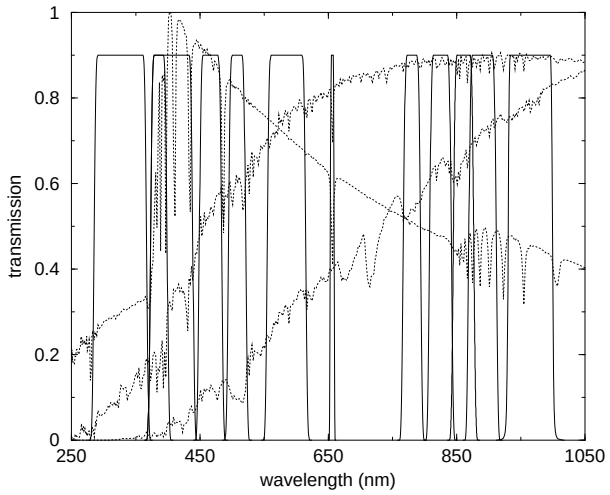

Figure 5. A current MBP proposal of 12 bands, named F7M (Jordi & Carrasco 2004b), is overplotted on the spectral energy distribution of A0 V, G2 V and K7 V type stars (dotted lines).

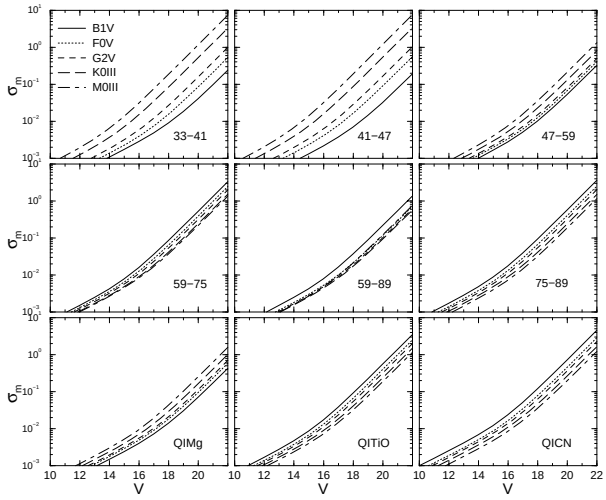

Figure 6. End-of-mission precision of several photometric indices obtained with the F7M system, without considering a minimum threshold error coming from the calibration of the mission. This minimum error is assumed to be about 3 mmag.

for M type stars and by a strong CN band for C-stars allowing TiO and CN abundances determination.

Current MBP systems proposals consist of 10 to 13 different filters with widths ranging from 10 to 80 nm. A current proposed system with 12 bands is shown in Figure 5. Briefly, the bands at ∼470, ∼585, ∼825, ∼890 and ∼965 nm measure pseudo-continua for most of the stars; the bands at ∼325, ∼385 and ∼410 nm are located in the wavelength range containing the information on chemical abundances for FGK-type stars, as stated above; the bands at ∼510 and 780 nm are centred in the Mg Ib triplet and the TiO absorption band, respectively; the ∼860 nm band covers the wavelength range of the radial-velocity spectrometer and finally, the band at 656 nm measures the strength of the H_α line that depends on temperature for early-type stars and that additionally allows to identify emission line stars. The Balmer and Paschen jumps, related with luminosity for early-type stars are well covered by the ∼325 and ∼410 nm bands and the ∼825 and ∼890 nm bands, respectively. Carbon stars are identified with the band at ∼825 nm. The associate end-of-mission errors for several colour indices are shown in Figure 6.

Intensive work is in progress to optimize the red bands for improving the reddening determination of intermediate type stars and the blue bands for investigating the α-elements abundance determination. Tautvaišienė & Edvardsson (2002) made a raw estimation of the precisions that could be obtained for α/Fe abundance determination. They obtained uncertainties of about 0.2 dex for G and K giants with $V \sim 18$ and dwarfs with $V \sim 16.5$ for thick disc stars if bands of about 8 – 10 nm were placed on the Ca II H and K lines and Mg Ib triplet, taking advantage of the inverse behaviour of the Ca II and Mg changing values of [Fe/H] and [α/Fe]. However, it is unlikely that photometry can provide α-elements abundances for the faintest giants and dwarfs observed by Gaia.

5. PHOTOMETRY PERFORMANCES

The evaluation of the photometric capabilities follows several steps described in the next sections.

5.1. Definition of Test Population

For every galactic stellar population and according to the scientific goals of Gaia, several kinds of stars were selected as Scientific Targets and a priority was assigned to them (Jordi et al. 2004a). These stars have been considered at different directions in the Milky Way and at different distances, according to a Galaxy Model (Torra et al. 1999) and they have been reddened according to a 3D interstellar absorption model (Drimmel et al. 2003) and assuming a standard extinction law. This results in a set of about 6500 targets each one with its estimated parallax error according to the colour and the apparent magnitude. The targets in the halo are considered to have [Fe/H] abundances from -4 to -1 dex and [α/Fe] abundances from 0.2 to 0.4 dex; for the thick disc targets we assumed [Fe/H] from -1 to 0 dex and [α/Fe] $= 0.2$ dex; for the thin disc targets, [Fe/H] from -1 to $+0.5$ dex and [α/Fe] -0.2 to 0.0 dex, and, finally, for the bulge targets, we assumed [Fe/H] as for the thin disc and [α/Fe] from 0 to 0.4 dex.

5.2. Simulated Photometry

For the simulation of synthetic white light (G), BBP and MBP fluxes and their corresponding error, spectral energy distributions (SEDs) for the scientific targets in the test population were taken from BaSeL (Lejeune et al. 1998), NextGen (Hauschildt et al. 1999) and MARCS

(Gustafsson et al. 2004) libraries. The well known BaSeL library covers the whole HR diagram and [M/H] abundances from -5 to $+1$ dex, but it does not consider [α/Fe] abundances different from solar. A new version of NextGen library is being built taking into account Gaia mission needs (Hauschildt et al. 2003). This library includes SEDs for stars cooler than 10 000 K with [M/H] ranging from -2 to $+0$ dex and [α/Fe] from -0.2 to $+0.4$ dex. Finally, a new version of MARCS library also taking into account non-solar α-elements abundances for Gaia purposes, provides coverage for $T_{\rm eff}$ between 3000 K and 5000 K, [M/H] from -4 to $+0.5$ dex and [α/Fe] from $+0$ to $+0.4$ dex.

The end-of-mission magnitude errors were computed taking into account the signal-to-noise ratio, the sky background contribution, the RON and the mean total number of observations, plus a margin error from unknown sources of 20%. The calibration errors introduce a minimum threshold magnitude error that we assumed to be 3 mmag for the end of mission. The results of the Photometric Data Analysis (Brown 2005) will better assess the value of this threshold.

5.3. Uncertainties of Astrophysical Parameters

Following Lindegren (2003b), consider the astrophysical parameters determination as a linearized least-squares estimation of $\mathbf{\Delta}\vec{\mathbf{p}}$, with $\vec{p}$ the vector of k astrophysical parameters, where the observation equation resulting from the normalized flux ϕ measured in filter j ($j = 1, n$ bands) is:

$$\sum_{i=1,k} \frac{\partial \phi_j}{\partial p_i} \Delta p_i = \Delta\phi_j \pm \epsilon_j \qquad (1)$$

where $\Delta\phi_j = \phi_{j,\rm obs} - \phi_j(\vec{p})$ is the $O-C$ in flux and $\pm$ indicates the flux uncertainty. The $\partial\phi_j/\partial p_i$ values constitute a *sensitivity matrix*, $\mathbf{S}$, of $n \times k$ elements. Observation equations of unit weight are formed through division by ϵ_j, whereupon normal equations are formed in the usual manner. The covariance of the estimated vector, $\vec{p}_{\rm post}$, is then given by the inverse of the normal equations matrix:

$$\mathbf{C}_{\vec{p}_{\rm post}} = \left(\mathbf{B} + \mathbf{S}^{\rm T}\mathbf{C}_{\phi}^{-1}\mathbf{S}\right)^{-1} \qquad (2)$$

The matrix $\mathbf{B}$ is a positive definite matrix with the *a priori* information of the astrophysical parameters vector $\vec{p}$ and it is introduced to avoid infinite or very large values of the elements in $\mathbf{C}_{\vec{p}_{\rm post}}$ caused by the degeneracy among the astrophysical parameters. In the absence of any other information, the *a priori* information is given by the range of possible values of the p_i parameters, $\mathbf{B} = {\rm diag}(\sigma_{i,\rm prior}^{-2})$. In this paper, the information coming from the parallax and its error has been introduced in this *a priori* matrix information, following Lindegren (2004). Other information could be added (known reddening in a certain galactic location, ranges of abundances according to galactic populations, ...). When the photometric system does not provide any relevant information on a given astrophysical parameter p_i (either because of the flux variances in $\mathbf{C}_{\phi}$ are too large or because the elements of the sensitivity matrix $\mathbf{S}$ are too small), then $\sigma_{i,\rm post} \simeq \sigma_{i,\rm prior}$.

The mean $\sigma_{T_{\rm eff},\rm post}/T_{\rm eff}$, $\sigma_{A_v,\rm post}$, $\sigma_{\log_g,\rm post}$ and $\sigma_{\rm [M/H],post}$ by groups of targets and for three directions in the Galaxy are shown in Figures 7 to 9. The figures are for the case of using the BaSeL2.2 SEDs library and combining white light, BBP and MBP fluxes with parallax information. The fluxes measured at the different

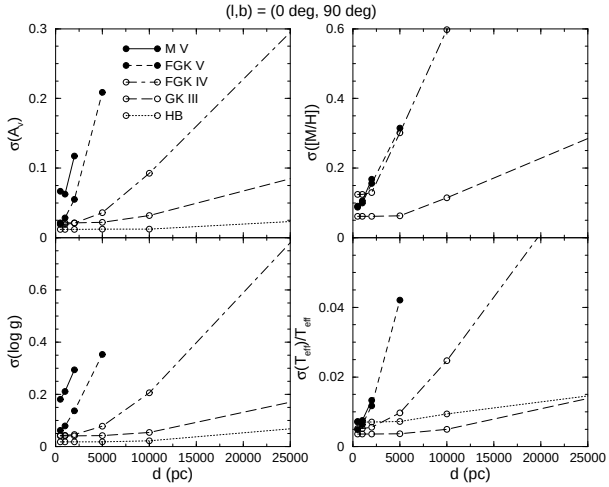

Figure 7. Estimation of the precisions of the main astrophysical parameters in the Galactic pole direction for several groups of stars. The interstellar absorption is assumed to reach 0.3 mag at 1 kpc and to be constant from this distance.

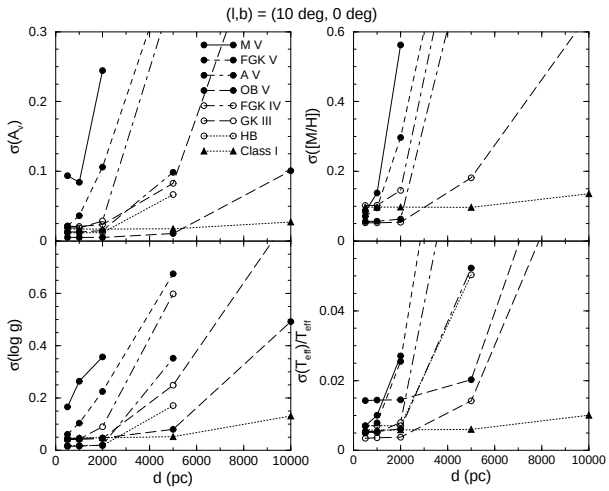

Figure 8. Estimation of the precisions of the main astrophysical parameters in the plane and Galactic center direction. Interstellar absorption is assumed to vary from 0.3 mag at 500 pc to 10 mag at 10 kpc. (Class I means luminosity class I).

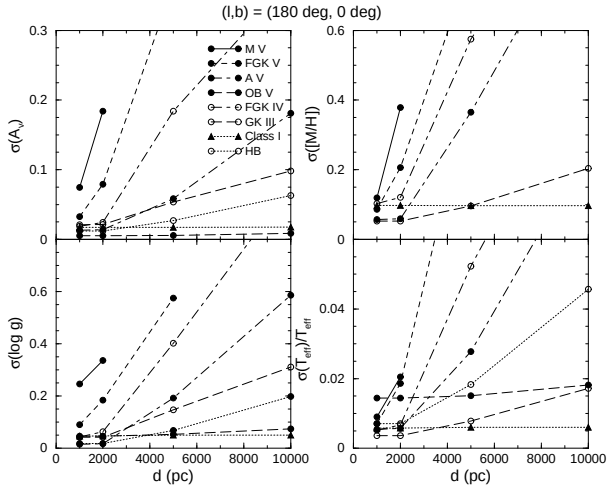

Figure 9. Estimation of the precisions of the main astrophysical parameters in the plane and Galactic anticenter direction. Interstellar absorption is assumed to vary from 0.3 mag at 500 pc to 3.5 mag at 5 kpc and to be constant from this distance.

bands are assumed to vary only due to changes in $T_{\rm eff}$, A_v, $\log_g$ and [M/H]. Different libraries predict different $\sigma_{i,\rm post}$ values, being the largest differences for cool stars (below 4000 K), for which Kurucz atmosphere models are not appropriate.

The bulge stars are faint because of the distance and the high reddening. In areas of low reddening, as in Baade's window, the stellar density is large and the MBP photometry will not be available. In that case, the derivation of stellar parameters from only G, BBP photometry and parallax is less precise. In spite of this, the estimated $\sigma_{A_v,\rm post}$ ranges from 0.2 to 0.6 mag, $\sigma_{T_{\rm eff},\rm post}/T_{\rm eff}$ from 1 to 10% and $\sigma_{\log_g,\rm post}$ from 0.1 to 0.5 dex, depending on the spectral type. In the case of highly reddened areas, the stellar density allows MBP measurements, and although the stars are very faint the estimated precision of the astrophysical parameters is still acceptable: $\sigma_{A_v,\rm post}$ ranges from 0.4 to 1.0 mag, $\sigma_{T_{\rm eff},\rm post}/T_{\rm eff}$ from 2 to 15% and $\sigma_{\log_g,\rm post}$ from 0.3 to 0.7 dex.

The obtained uncertainties in the parameters may seem too optimistic, but they are not necessarily so. On one side it is true that the estimation of the $\sigma_{i,\rm post}$ in the way explained above assumes that the changes in the measured fluxes of a given star, and hence the changes in its SED, are only due to changes of the p_i parameters in $\vec{p}$. It also assumes that the changes of the SEDs with the p_i parameters, i.e. $\partial\phi_j/\partial p_i$, match the changes of the true stars. In other words, cosmic dispersion (the effects of rotational velocity, magnetic fields, chemical composition differences element by element, differences on the interstellar extinction law and so on) and inaccuracies of the SEDs libraries are not taken into account. An additional source of uncertainty comes from the classification and parametrization algorithms (see Bailer-Jones (2005)). The uncertainties due to the algorithms themselves, because of non full efficiency and lack of knowledge of the true stellar astrophysics, is not taken into account either in the present formalism.

But, on the other hand it is also true that Gaia photometry provides about 17 colour indices for every observed target, to which the information coming from the parallax has to be added. There is no precedent for deriving stellar astrophysical parameters in such a way.

Therefore, although the $\sigma_{i,\rm post}$ here are the maximum precision that can be obtained, we estimate that the main uncertainty will come from the imperfect knowledge of the SEDs of the true stars and not be due to an imperfect design of the photometric system.

6. GALAXY STRUCTURE AND EVOLUTION STUDIES

The 'Gaia Concept and Technology Study Report' (ESA 2000) defines the Gaia science case and the main tracers of every topic. A brief and incomplete list of those concerning Galactic structure and evolution are:

1– Chemical abundance galactocentric distribution: G and K giants
2– Age galactocentric gradients, SFR: HB stars, early-AGB, MS turn-off stars
3– Disentangling age-metallicity degeneracy: MS turn-off, subgiants
4– Star formation history: MS stars earlier than G5V, subgiants
5– Detailed knowledge of LF: low MS stars
6– Halo streams, age and chemical abundance determinations: G and K giants
7– Outer halo ($R > 20$ kpc), accretion and merging: G and K giants and HB stars
8– Earliest phases of evolution of the Galaxy: most metal-poor stars, C- subgiants and dwarfs near the turn-off
9– Distance scale: RR-Lyrae, Cepheids
10– Thick disc formation mechanism (pre- *vs* post-thin disc): G and K giants, HB stars
11– Merging and/or diffusion: high velocity A-type stars
12– 'in situ' gravitational potential, K_z, age-velocity relation: F-G-K dwarfs
13– Large scale structure (warp, asymmetry): K-M giants
14– Interstellar medium distribution: O-F dwarfs
15– Large scale structure (spiral arms, star-formation regions): OB stars, supergiants
16– Star formation rate in the bulge: RGB, AGB
17– Shape of the bulge, orientation, bar: RGB, AGB, Red clump stars

Groups of stars in Figures 7–9 correspond to these scientific topics.

6.1. Chemical Abundances

The 2001 version of the [Fe/H] catalog by Cayrel de Strobel et al. (2001) compiles high-resolution, high S/N ratio spectroscopic determinations of [Fe/H] for F, G and K

stars. The typical $\sigma_{[\mathrm{Fe/H}]}$ for the stars with several measurements is 0.10 – 0.15 dex, although several ones reach 0.4 dex.

Figures 7 to 9 show that Gaia photometry is able to match the spectroscopic precision up to about 1 – 2 kpc from the Sun depending on the Galactic direction (i.e., the reddening) for F–M dwarfs and subdwarfs. For giants in the red clump and the red giant branch, being brighter, the same precision is attainable up to about 4, 7 and 12 kpc in the center, anticenter and orthogonal galactic directions, respectively. This result ensures: a) the determination of the chemical abundance galactocentric gradient, b) the classification of the stars as belonging to different stellar populations, c) the characterization of halo streams (a KIII giant at 30 kpc carries an uncertainty of $\sigma_{[\mathrm{M/H}],\mathrm{post}} = 0.2$ dex if [M/H]$\sim$ -2 and 0.4 dex if [M/H]$= -4$), d) the distance scale through the metallicity determination of RR-Lyrae, among other goals.

As usual, low metallicities are more poorly determined than solar or higher metallicities. Cool unresolved binaries tend to mimic a single star with less metal content. As an example, G and K dwarfs with companions fainter by 1.5$-$2 mag yield to Δ[M/H]~ -0.4. This bias decreases to Δ[M/H]$\sim$ -0.2 when $\Delta m = 3$.

6.2. Interstellar Extinction and Effective Temperature

The determination of effective temperatures (or intrinsic colours) and absolute magnitudes requires accurate determinations of interstellar extinction and the interstellar extinction law. If a standard extinction law is assumed, optical photometry allows the direct determination of the individual reddening for main sequence early-type stars (see Figures 8 and 9), but not for the late-type stars, because A_{v} and T_{eff} determinations are degenerate. Additional information for late-type stars is then needed.

Due to the very uneven distribution of dust in all three dimensions, an account of reddening by some kind of sky map is impossible, especially at low galactic latitudes. Meanwhile the extinction law also varies across the Galaxy due to different chemical compositions and/or different size distributions of the dust (Fitzpatrick 1999; Draine 2004). The extinction law in the optical is primarily a function of the size distribution of the dust. Variations in the extinction law in the NIR may be due to metallicity effects, but these variations are much smaller than those in the optical and not necessarily correlated. To go from A_K to A_V one will still need some independent indication of the extinction law in the optical, or assume a standard extinction law.

In addition to the diffuse interstellar band at 862 nm, located in the wavelength range covered by the RV spectrograph, the equivalent width of the calcium triplet, in combination with a reddening-free colour index formed from a medium and broad band with 'identical' central wavelengths, can be used to estimate the extinction.

During the luminosity calibration of 2MASS photometry for A9–K5 main sequence stars, Knude & Fabricius (2003) noticed significant reddening vectors in the M_J vs. $(J-H)_{\mathrm{obs}}$ diagram where M_J was estimated from Hipparcos parallaxes $\pi > 8.0$ mas and $\sigma_\pi/\pi < 0.11$, assuming that reddening was negligible. Vectors are most pronounced for the A type stars but are also present for cooler ones. From these vectors the reddening law may be estimated even for various spectral classes if the stellar density is large enough. Similar diagrams may be constructed from Gaia astrometry and BBP and MBP for the optical region and for the infrared from 2MASS, UKIDSS and VISTA surveys so that regions with abnormal extinction can be identified.

Effective temperatures with an uncertainty of $\sim$ 2% are achievable for all observable red giants in the halo and most of them in the galactic plane. For cool dwarfs, being fainter, this is true for distances shorter than 2 kpc. For early dwarfs, being bright and with a well determined reddening, the achievable distance for the 2% error is about 4 and 10 kpc in the galactic center and anticenter direction, respectively.

6.3. Absolute Luminosity and Surface Gravity

Photometry will be crucial for the determination of absolute luminosities (or surface gravities) in the case of large parallax relative error ($>10-20$%). Absolute magnitude calibrations could be established with the good parallax stars and applied to more distant stars in the traditional way, assuming that they are intrinsically similar to the good parallax stars, which may not always be the case. Thus, luminosities at the level of $\sigma_{M_V} \sim 0.2-0.4$ mag (or $\sigma_{\log g} \sim 0.1-0.2$ ex) from photometry is desirable to match the accuracy of the well measured parallaxes.

Figures 7 to 9 show that at large distances, gravity determination of giants and early-type stars will allow the study of the large scale structure of the warp, spiral arms, mapping the star-formation regions and so on.

6.4. Age

As it is well-known, the location of a star in the HR diagram does not allow to unequivocally determine the age (several combinations of [Fe/H], [α/Fe] and age are possible). Individual accurate ages would require extremely accurate determination of temperatures, reddening and chemical composition, and Gaia will do so.

For ages around $10-14$ Gyr, an age variation of 2 Gyr yields a variation of the log T_{eff} turn-off of about 0.01 dex for a given chemical composition. The same variation is derived when an uncertainty of 0.3 dex in [Fe/H] is considered for a fixed age. The variation of the α-elements abundance has a smaller impact on the age determination than the variation of [Fe/H]. In summary, an uncertainty of about $4-5$ Gyr is estimated for the individual ages from subgiants and stars in the turn-off of halo, thick and old-thin disc stars up to about 2, 3 and 5 kpc in the galactic center, anticenter and orthogonal directions, respectively. As usual, subsets of each galactic population

(such as globular clusters, open clusters, OB associations, a given halo stream, an identified merger, etc.) can be treated statistically and ages and metallicities of the subset can be obtained with much better precisions than those of the individual members.

The age galactocentric gradient, the star formation history, the disentangling of the age-metallicity degeneracy, the thick disc formation mechanism and so on, are fully assured from the present expectations.

7. PRESENT WORK

The present BBP and MBP photometric systems already assure the Gaia scientific objectives. However, improvement is still possible and an intensive work is ongoing in the Photometry Working Group investigating the [α/Fe] abundance determination and the inclusion of a process of evaluation of the performances for emission line stars and peculiar stars detection, Solar System objects, QSO, etc. A procedure for the photometric systems evaluation is defined in Brown et al. (2004) allowing the identification of merits and drawbacks of every proposal and the convergence up to a unique photometric system.

ACKNOWLEDGMENTS

The design of the Gaia photometric system is based on years of work in the Photometry Working Group which has 49 core members and 25 associates. C. Jordi acknowledges MCYT for its financial support under contract PNE2003-04352.

REFERENCES

Bailer-Jones, C. 2004, A&A 419,385

Bailer-Jones, C. 2005, ESA SP-576, this volume

Brown, A., 2005, ESA SP-576, this volume

Brown, A., Jordi, C., Knude, J., Høg, E., 2004 Gaia technical report PWG–AB–003

Cayrel de Strobel, G., Soubiran, C., Ralite, N., 2001 A&A 373, 159

Draine B.T., 2004, in 'Origin and Evolution of the Elements', McWilliam A. & Rauch M., eds., p. 320

Drimmel, R. Cabrera-Lavers, A., López-Corredoira, M., 2003, A&A 409, 205

ESA, 2000, Gaia: Composition, Formation and Evolution of the Galaxy, ESA-SCI(2000)4

Fitzpatrick, E.L., 1999, PASP 111, 63

Grenon, M., Jordi, C., Figueras, F., Torra, J. 1999, Gaia technical report MGUB–PWG–002

Gustafsson et al., 2004, in preparation

Hauschildt, P.H., Allard, F., Baron, E., 1999, ApJ 512, 377

Hauschildt, P.H., Allard, F., Baron, E., Aufdenberg, J., Schweitxer A., 2003, in 'GAIA Spectroscopy, Science and Technology', Munari, U. ed., ASP Conf. Ser., vol. 298, p. 179

Heiter, U., Piskunov, N., Gustafsson, B., Jordi, C., Carrasco, J.M., 2004, in '13th Cool Stars Workshop', in press

Høg, E. 2004a, Gaia technical report GAIA–CUO–150

Høg, E. 2004b, Gaia technical report GAIA–CUO–151

Jordi, C., Figueras, F., Carrasco, J.M., Knude, J., 2004a, Gaia technical report UB–PWG–009

Jordi, C., Figueras, F. Torra, J., Carrasco, J.M. 2004b, Gaia technical report UB–PWG–016

Jordi, C., Carrasco, J.M., 2004a, Gaia technical report UB–PWG–026

Jordi, C., Carrasco, J.M., 2004b, Gaia technicalreport UB–PWG–027

Knude J., Fabricius C., 2003, Baltic Astronomy 12, 508

Knude, J. Høg, E. 2004, Gaia technical report GAIA–CUO–148

Lejeune, T., Cuisinier, F., Buser, R., 1998, A&AS 130,65

Lindegren, L. 2003a, Gaia technical report GAIA–LL–045

Lindegren L., 2003b, Gaia technical report GAIA–LL–047

Lindegren L., 2003c, Gaia technical report GAIA–LL–049

Lindegren, L. 2004, Gaia technical report GAIA–LL–054

Munari, U. 1999, Baltic Astronomy, 8, 123

Straižys, V. 2004, Gaia technical report GAIA–VILN–002

Straižys, V., Zdanavicius, K., Lazauskaite, R., 2004, Gaia technical report GAIA–VILN–001

Tautvaišienė, G., Edvardsson, B. 2002, ApSS 280, 143

Torra, J., Chen, B., Figueras, F., Jordi, C., Luri, X., 1999, Baltic Astronomy, 8, 171

Vansevicius, V., & Bridzius, A., 2003, in 'GAIA Spectroscopy, Science and Technology', Munari, U. ed., ASP Conf. Ser., vol. 298, p. 41